

Complex constraints on allometry revealed by artificial selection on the wing of *Drosophila melanogaster*

Geir H. Bolstad^{a,b,c,1}, Jason A. Cassara^c, Eladio Márquez^c, Thomas F. Hansen^d, Kim van der Linde^c, David Houle^c, and Christophe Pélabon^b

^aNorwegian Institute for Nature Research, 7485 Trondheim, Norway; ^bCentre for Biodiversity Dynamics, Department of Biology, Norwegian University of Science and Technology, 7491 Trondheim, Norway; ^cDepartment of Biological Science, Florida State University, Tallahassee, FL 32306; and ^dDepartment of Biology, CEES & EVOGENE, University of Oslo, 0316 Oslo, Norway

Edited by James H. Brown, University of New Mexico, Albuquerque, NM, and approved August 18, 2015 (received for review March 17, 2015)

Precise exponential scaling with size is a fundamental aspect of phenotypic variation. These allometric power laws are often invariant across taxa and have long been hypothesized to reflect developmental constraints. Here we test this hypothesis by investigating the evolutionary potential of an allometric scaling relationship in drosophilid wing shape that is nearly invariant across 111 species separated by at least 50 million years of evolution. In only 26 generations of artificial selection in a population of *Drosophila melanogaster*, we were able to drive the allometric slope to the outer range of those found among the 111 sampled species. This response was rapidly lost when selection was suspended. Only a small proportion of this reversal could be explained by breakup of linkage disequilibrium, and direct selection on wing shape is also unlikely to explain the reversal, because the more divergent wing shapes produced by selection on the allometric intercept did not revert. We hypothesize that the reversal was instead caused by internal selection arising from pleiotropic links to unknown traits. Our results also suggest that the observed selection response in the allometric slope was due to a component expressed late in larval development and that variation in earlier development did not respond to selection. Together, these results are consistent with a role for pleiotropic constraints in explaining the remarkable evolutionary stability of allometric scaling.

allometry | artificial selection | comparative analyses | developmental constraints | pleiotropy

Allometric scaling is a ubiquitous aspect of biological variation that is often strongly conserved across evolutionary time and typically explains a large fraction of observed variation in morphology, physiology, or life history (1–7). This evolutionary conservatism can be explained either by stabilizing selection or by developmental or physiological constraints (8–17). Allometric power laws have been thought to reflect developmental constraints for nearly a century (6). Arguments of allometric constraints were used to explain patterns of macroevolution by architects of the modern synthesis such as Huxley (5), Simpson (18), and Rensch (19), and played a major role in Gould and Lewontin's (20) criticism of the "adaptationist programme." The idea of allometric constraints may, at least partially, have originated from the multiplicative growth model underlying Huxley's derivation of the allometric power law for morphological traits.

Julian Huxley (5, 21) showed that when a trait is under common growth regulation with size, the relationship between the trait Y and a size measure X is a power function of the form $Y = aX^b$, where a and b are constants. On a log–log scale, power functions become linear, with $\log(a)$ representing the intercept and b representing the slope of the allometric relationship $\log(Y) = \log(a) + b \log(X)$. Allometric power laws summarize variation among developmental stages (ontogenetic allometry), individuals in a population (static allometry), and populations or species (evolutionary allometry) (22). The three levels of allometry are related, and a higher level of allometry can be expressed as a function of allometry at lower levels (23). Limited potential for evolution at a

lower level in this allometric hierarchy would then cause constraints at all higher levels (6, 23).

Because of their fundamental importance and their relation to developmental constraints, there has been interest in testing the evolvability of scaling relationships in general and, in particular, the evolvability and evolutionary invariance of the static allometric slope. In a recent review, Voje et al. (6) argued that, although there is abundant evidence for evolvability of intercepts of static allometric relations (i.e., mean shape), there are few clear demonstrations of additive genetic variance or microevolutionary changes in allometric slopes. Although there are many claims of evolvable allometric slopes in the literature, most are problematic due to various conceptual and methodological issues (see refs. 6 and 24–26).

One exception is Pavlicev et al.'s (27) finding of small but significant heritabilities for several allometric exponents in an intercross between mouse strains selected for large and small body size. Another case comes from Tobler and Nijhout (28), where 10 generations of selection on wing mass in the moth *Manduca sexta* produced a small change in wing–body scaling (see ref. 6 for a reanalysis). This was, however, an indirect response, so it is unclear how free the slope was to evolve on its own. The result is also based on observing the relationship in a single generation, calling its replicability into question (see ref. 26 for further discussion). In the only study that performed artificial selection separately and directly on the allometric slope and intercept, Egset et al. (29) found a clear response in the intercept but not in the slope of a tail–body allometry in guppies (*Poecilia reticulata*). The power of this study was also limited, however, because it extended only over three generations. From

Significance

Many traits scale precisely with size, but it is unknown whether this is due to selection for optimal function or due to evolutionary constraint. We use artificial selection to demonstrate that wing-shape scaling in fruit flies can respond to selection. This evolved response in scaling was lost during a few generations after selection ended, but other selected changes in wing shape persisted. Shape–size scaling in fly wings is therefore evolvable, but adaptation is apparently constrained by selection that may not be on wings. This may explain why scaling relationships are often evolutionarily conserved.

Author contributions: G.H.B., J.A.C., T.F.H., D.H., and C.P. designed research; J.A.C., E.M., K.v.d.L., and D.H. performed research; G.H.B. analyzed data; and G.H.B., J.A.C., T.F.H., D.H., and C.P. wrote the paper.

The authors declare no conflict of interest.

This article is a PNAS Direct Submission.

Data deposition: The data have been deposited in the Dryad Digital Repository, dx.doi.org/10.5061/dryad.s270f.

¹To whom correspondence should be addressed. Email: geir.bolstad@nina.no.

This article contains supporting information online at www.pnas.org/lookup/suppl/doi:10.1073/pnas.1505357112/-DCSupplemental.

disequilibrium. However, this does not completely prevent association between alleles, and we need to consider if the reversal of the response could have been due to breakup of linkage disequilibrium. Assuming an average recombination fraction of $r = 0.365$ between random loci in *D. melanogaster* (37), we estimated that the maximum fraction of the response that could be due to linkage disequilibrium averaged only $19.9 \pm 22.6\%$ and $14.3 \pm 24.0\%$ in males and females, respectively.

Nongenetic inheritance, such as parental (e.g., maternal) effects, may, in principle, affect the response to selection (38) but is not likely to be important in this case, as there are no indications of heritable nongenetic effects on wing shape in drosophilids.

We consider natural selection to be the most likely cause of the reversal toward the ancestral allometric slope. However, natural selection for restoring optimal wing function, for example due to selection for flight or courtship behavior, does not seem to be strong in the laboratory environment. In the presence of such selection, we expect that the intercept-selected populations would also have rapidly returned to their starting value. These populations instead showed little reversal of the selection response over an even longer time period, despite being more different from the initial wing shape than the slope-selected populations. Therefore, the more likely alternative is that the evolutionary change in allometric slope generated deleterious pleiotropic responses in other aspects of the phenotype, resulting in strong natural selection in the laboratory environment.

We have shown that a phylogenetically nearly invariant allometric slope can evolve rapidly under selection, but that this seems to generate countervailing natural selection to return the allometric slope to its initial value. This suggests that conserved allometric scaling may be best explained by pleiotropic constraints (12). Riedl (39, 40) proposed that fundamental developmental processes may become increasingly constrained, or burdened, by other processes that interact with or depend on them. Under this hypothesis, aspects of the developmental system that lead to precise allometric scaling also affect other aspects of organismal form and function, leading to deleterious pleiotropic effects when they are altered. If true, this hypothesis could provide a general explanation for the striking evolutionary conservatism of allometric power laws, while still leaving open the possibility for allometries to be optimized by natural selection over long time scales through compensatory mutations.

Materials and Methods

Comparative Data. Species were obtained by collection from the wild, from the *Drosophila* Species Stock Center, or from other collectors. The full list of 111 taxa, specifications, their collection locations, and sample sizes are reported in Table S6. Flies were reared using combinations of food, temperature, and rearing environments suggested to be optimal for each particular species based on the instructions from the source or from published sources. Wild-collected specimens were measured when we were unable to rear the flies in the laboratory. Most of the 111 taxa are currently classified in the paraphyletic genus *Drosophila* or to genera in the subfamily Drosophilinae (41, 42). In addition, we included two species of steganine drosophilids and five outgroup species from other families. Four drosophilid species are represented by more than one subspecies. Most species had sample sizes of around 200 measured flies, and the total sample size was 20,345.

Wing Measurements. The full procedure for imaging wings and for estimating vein locations and corresponding landmarks has been described by Houle et al. (43). In short, the left wing of a live CO₂-anesthetized fly is immobilized in a suction device, a digital image of the wing is obtained, and the program Wings3.8 (44) is used to fit cubic B-splines to the wing veins, from which the coordinates of landmarks and semilandmarks are extracted. The length of vein L2 was estimated as the straight-line distance between the humeral break in the costa and the distal end of L2. The square root of wing area was used as a measure of wing size. See Fig. S3 for detailed information on the wing measurements.

Derivation of Populations for the Selection Experiment. The initial population was made by intercrossing 30 inbred lines obtained from the *Drosophila* Genetic Reference Panel (45). This population was allowed to mate freely for one generation before being divided into the selected populations. We maintained 16 different populations in this experiment: two selected for increase and two for decrease in allometric intercept, two for increase and two for decrease in allometric slope, two for increase and two for decrease in slope with the starvation treatment, and two unstarved and two starved controls. Details are given in SI Materials and Methods.

Rearing of Selected Populations. Details are given in SI Materials and Methods.

Justification of the Allometric Slope Selection Index. Details are given in SI Materials and Methods.

Selection Procedure. In the two replicate control populations, 20–25 virgin females and 20–25 males were chosen haphazardly and imaged before being divided into two vials to produce the next generation.

In the two replicate starved control populations, 50 virgin females and 50 males were imaged, then divided haphazardly into four groups of 25 flies each (12 or 13 of each sex). Two groups were placed in vials and their larvae fed normally; the other two were placed in “egg layers,” and their larvae underwent the starvation treatment (see SI Materials and Methods). Note that these two populations were started later in the experiment (at generation 5 of the other populations).

Two replicate populations were maintained for each direction (up and down) of selection on the allometric intercept. Each generation in each population, 100 virgin females and 100 males were chosen haphazardly and imaged. From these, 20–25 of each sex were selected to produce the next generation, using the selection index

$$W_{int} = \beta_1(x - \bar{x}) + \beta_2(y - \log_e[a] - bx),$$

where x is \log_e wing size (square-root wing area), \bar{x} is the average of x , y is \log_e L2 length, $\log_e[a]$ is the allometric intercept, b is the allometric slope, and the term $(y - \log_e[a] - bx)$ is the residuals of the allometric regression. For the up selection, $\beta_2 = 1$, and for the down selection, $\beta_2 = -1$, whereas β_1 was optimized to reduce selection on size (see SI Materials and Methods). The selection index was fitted independently each generation within each selected population, and the flies were stored in individual vials from imaging until the selection index score of each fly was calculated. Selection on the intercept was maintained in both replicates (A and B) for seven generations for both the up and the down directions. After this, the A replicates were discarded, whereas up- and down-selected populations in replicate B were maintained with relaxed selection (i.e., the same mating regime as in the control populations) for an additional 16 generations.

For each direction (up and down) of selection on the allometric slope, we kept two replicate populations (A and B). Each generation in each population, 100 virgin females and 100 males were imaged, of which 24 were selected using the selection index

$$W_{slope} = \beta_x(x - \bar{x}) + \beta_y(y - \bar{y}) + \frac{1}{2}\gamma_x(x - \bar{x})^2 + \gamma_{xy}(x - \bar{x})(y - \bar{y}),$$

where $\gamma_{xy} = 1$ for the up selection (increase in slope) and -1 for the down selection (decrease in slope). This function was optimized by choosing values of the parameters β_x , β_y , and γ_x to minimize selection on the means of x and y and on the variance of x (see SI Materials and Methods). The selection index was fitted independently each generation within each selected population, and the flies were stored in individual vials after imaging until the selection index score of each fly was calculated. To prevent linkage disequilibrium, we enforced disassortative mating on size by first dividing the selected flies into two groups, one containing the largest 12 females and smallest 12 males, the other with the smallest 12 females and largest 12 males. Each of these groups was then split at random into two groups of six males and six females, and each such group was placed in vials with another group of opposite-sex flies of contrasting size. These flies were allowed to mate and lay eggs overnight. Selection was carried out for 26 generations in replicate A and for 25 generations in replicate B. After this, we maintained the populations for an additional 13 generations in replicate A and 14 generations in replicate B under relaxed selection (i.e., the same mating regime as the control populations). At generation 23, we split off a population from each of the replicates and maintained these new populations under relaxed selection for 15 generations. At several points during the period of relaxed selection, we imaged 100 males and 100 females from each of the populations (see Fig. 2B).

We also maintained two replicate starved slope-selected populations for each direction of slope selection. These were subjected to the same selection regime as the unstarved slope-selected populations but reared using the starvation treatment. Selection was carried out for 19 generations in these populations. Details are given in *SI Materials and Methods*.

Statistical Analyses. To estimate the rate of evolution for the allometric intercept and slope, we fitted a Brownian-motion model of evolution using a phylogenetic mixed model (46). Because the depth of the phylogeny is highly uncertain (47), we used both a best guess of 133 million years and a conservative estimate of 50 million years to estimate the rate.

1. Charnov EL (1993) *Life History Invariants* (Oxford Univ Press, New York).
2. Schmidt-Nielsen K (1984) *Scaling: Why Is Animal Size So Important?* (Cambridge Univ Press, Cambridge, UK).
3. West GB, Brown JH, Enquist BJ (1997) A general model for the origin of allometric scaling laws in biology. *Science* 276(5309):122–126.
4. Brown JH, West GB (2000) *Scaling in Biology* (Oxford Univ Press, Oxford).
5. Huxley JS (1932) *Problems of Relative Growth* (MacVeagh, New York).
6. Voje KL, Hansen TF, Egset CK, Bolstad GH, Pélabon C (2014) Allometric constraints and the evolution of allometry. *Evolution* 68(3):866–885.
7. Gould SJ (1966) Allometry and size in ontogeny and phylogeny. *Biol Rev Camb Philos Soc* 41(4):587–640.
8. Bradshaw AD (1991) The Croonian Lecture, 1991. Genostasis and the limits to evolution. *Philos Trans R Soc Lond B Biol Sci* 333(1267):289–305.
9. Björklund M (1996) The importance of evolutionary constraints in ecological time scales. *Evol Ecol* 10(4):423–431.
10. Schluter D (2000) *The Ecology of Adaptive Radiation* (Oxford Univ Press, Oxford).
11. Arnold SJ, Pfrender ME, Jones AG (2001) The adaptive landscape as a conceptual bridge between micro- and macroevolution. *Genetica* 112–113:9–32.
12. Hansen TF, Houle D (2004) Evolvability, stabilizing selection, and the problem of stasis. *Phenotypic Integration: Studying the Ecology and Evolution of Complex Phenotypes*, eds Pigliucci M, Preston K (Oxford Univ Press, Oxford), pp 130–150.
13. Brakefield PM, Roskam JC (2006) Exploring evolutionary constraints is a task for an integrative evolutionary biology. *Am Nat* 168(6):54–513.
14. Polly PD (2008) Developmental dynamics and G-matrices: Can morphometric spaces be used to model phenotypic evolution? *Evol Biol* 35(2):83–96.
15. Futuyma DJ (2010) Evolutionary constraint and ecological consequences. *Evolution* 64(7):1865–1884.
16. Hansen TF (2012) Adaptive landscapes and macroevolutionary dynamics. *The Adaptive Landscape in Evolutionary Biology*, eds Svensson EI, Calsbeek R (Oxford Univ Press, Oxford), pp 205–226.
17. Bolstad GH, et al. (2014) Genetic constraints predict evolutionary divergence in *Dalechampia* blossoms. *Philos Trans R Soc Lond B Biol Sci* 369(1649):20130255.
18. Simpson GG (1944) *Tempo and Mode in Evolution* (Columbia Univ Press, New York).
19. Rensch B (1959) *Evolution Above the Species Level* (Columbia Univ Press, New York).
20. Gould SJ, Lewontin RC (1979) The spandrels of San Marco and the Panglossian paradigm: A critique of the adaptationist programme. *Proc R Soc Lond B Biol Sci* 205(1161):581–598.
21. Huxley JS (1924) Constant differential growth-ratios and their significance. *Nature* 114(2877):895–896.
22. Cheverud JM (1982) Relationships among ontogenetic, static, and evolutionary allometry. *Am J Phys Anthropol* 59(2):139–149.
23. Pélabon C, et al. (2013) On the relationship between ontogenetic and static allometry. *Am Nat* 181(2):195–212.
24. Houle D, Pélabon C, Wagner GP, Hansen TF (2011) Measurement and meaning in biology. *Q Rev Biol* 86(1):3–34.
25. Hansen TF, Bartoszek K (2012) Interpreting the evolutionary regression: The interplay between observational and biological errors in phylogenetic comparative studies. *Syst Biol* 61(3):413–425.
26. Pélabon C, et al. (2014) Evolution of morphological allometry. *Ann N Y Acad Sci* 1320: 58–75.
27. Pavlicev M, Norgard EA, Fawcett GL, Cheverud JM (2011) Evolution of pleiotropy: Epistatic interaction pattern supports a mechanistic model underlying variation in genotype-phenotype map. *J Exp Zool B Mol Dev Evol* 316(5):371–385.
28. Tobler A, Nijhout HF (2010) Developmental constraints on the evolution of wing-body allometry in *Manduca sexta*. *Evol Dev* 12(6):592–600.
29. Egset CK, et al. (2012) Artificial selection on allometry: Change in elevation but not slope. *J Evol Biol* 25(5):938–948.
30. Frankino WA, Zwaan BJ, Stern DL, Brakefield PM (2005) Natural selection and developmental constraints in the evolution of allometries. *Science* 307(5710):718–720.
31. Frankino WA, Zwaan BJ, Stern DL, Brakefield PM (2007) Internal and external constraints in the evolution of morphological allometries in a butterfly. *Evolution* 61(12): 2958–2970.
32. Weber KE (1990) Selection on wing allometry in *Drosophila melanogaster*. *Genetics* 126(4):975–989.
33. Wilkinson GS (1993) Artificial sexual selection alters allometry in the stalk-eyed fly *Cyrtodiopsis dalmanni* (Diptera, Diopsidae). *Genet Res* 62(3):213–222.
34. Emlen DJ (1996) Artificial selection on horn length-body size allometry in the horned beetle *Onthophagus acuminatus* (Coleoptera: Scarabaeidae). *Evolution* 50(3): 1219–1230.
35. Okada K, Miyatake T (2009) Genetic correlations between weapons, body shape and fighting behaviour in the horned beetle *Gnatocerus cornutus*. *Anim Behav* 77(5): 1057–1065.
36. Hallgrímsson B, et al. (2009) Deciphering the palimpsest: Studying the relationship between morphological integration and phenotypic covariation. *Evol Biol* 36(4): 355–376.
37. Lynch M, Walsh B (1998) *Genetics and Analysis of Quantitative Traits* (Sinauer Assoc, Sunderland, MA).
38. Kirkpatrick M, Lande R (1989) The evolution of maternal characters. *Evolution* 43(3): 485–503.
39. Riedl R (1977) A systems-analytical approach to macro-evolutionary phenomena. *Q Rev Biol* 52(4):351–370.
40. Riedl R (1978) *Order in Living Organisms: A Systems Analysis of Evolution* (Wiley, Brisbane, Australia).
41. van der Linde K, Houle D (2008) A supertree analysis and literature review of the genus *Drosophila* and closely related genera (Diptera, Drosophilidae). *Insect Syst Evol* 39(3):241–267.
42. van der Linde K, Houle D, Spicer GS, Steppan SJ (2010) A supermatrix-based molecular phylogeny of the family Drosophilidae. *Genet Res* 92(1):25–38.
43. Houle D, Mezey J, Galpern P, Carter A (2003) Automated measurement of *Drosophila* wings. *BMC Evol Biol* 3(1):25.
44. van der Linde K (2004–2013) Wings: Automated capture of *Drosophila* wing shape. Version 3.8. Available at bio.fsu.edu/~dhoule/wings.html. Accessed 2013.
45. Mackay TFC, et al. (2012) The *Drosophila melanogaster* genetic reference panel. *Nature* 482(7384):173–178.
46. Lynch M (1991) Methods for the analysis of comparative data in evolutionary biology. *Evolution* 45(5):1065–1080.
47. Obbard DJ, et al. (2012) Estimating divergence dates and substitution rates in the *Drosophila* phylogeny. *Mol Biol Evol* 29(11):3459–3473.
48. Stillwell RC, Dworkin I, Shingleton AW, Frankino WA (2011) Experimental manipulation of body size to estimate morphological scaling relationships in *Drosophila*. *J Vis Exp* (56):e3162.
49. O’Grady PM (1999) Reevaluation of phylogeny in the *Drosophila obscura* species group based on combined analysis of nucleotide sequences. *Mol Phylogenet Evol* 12(2):124–139.
50. R Core Team (2013) *R: A Language and Environment for Statistical Computing* (R Found Stat Comput, Vienna).
51. Bates D, Maechler M, Bolker B, Walker S (2013) lme4: Linear mixed-effects models using Eigen and S4. R package version 1.0-5. Available at <https://cran.r-project.org/web/packages/lme4/index.html>. Accessed 2013.
52. Bates D, Vazquez AI (2013) pedigreemm: Pedigree-based mixed-effects models. R package version 0.3-1. Available at <https://cran.r-project.org/web/packages/pedigreemm/index.html>. Accessed 2013.

Supporting Information

Bolstad et al. 10.1073/pnas.1505357112

SI Materials and Methods

Derivation of Populations for the Selection Experiment. The 30 inbred lines from the *Drosophila* Genetic Reference Panel (45) used to form the initial population were RAL 149, 324, 383, 486, 563, 714, 761, 787, 796, 801, 802, 804, 808, 819, 821, 822, 832, 843, 849, 850, 853, 859, 861, 879, 887, 897, 900, 907, 911, and 913. For the initial set of crosses, healthy lines were crossed with lines that were less fecund. Each cross, including reciprocals, was set up in six replicate vials of five or six females and three males. Virgin females and males were collected from the F₁ offspring, and the next round of pairwise crosses was set up once a sufficient number of flies had been obtained. This procedure was continued until a single population resulted.

To found the initial (Generation 0) populations subjected to intercept and slope selection, we sampled 100 flies of each sex from the base population. For each of the starved control starting populations, we sampled 50 flies of each sex, and, for each of the well-fed control starting populations, we sampled 40 flies of each sex.

Rearing of Selected Populations. Throughout the experiment, all of the selected populations (except those undergoing the starvation treatment; see below) were reared in 22-mm-diameter cylindrical vials containing ~4 mL of food medium composed of yeast, corn flour, sucrose, propionic acid, and agar, plus an antibiotic (cycled between streptomycin, penicillin, and tetracycline). Vials were stored in an incubator at 25 °C, 55–65% relative humidity, with a 12:12 h light/dark cycle. In all populations, flies were split into several vials for rearing, with roughly equal numbers of males and females. The number of adult flies in each vial was kept sufficiently low (less than 13 flies of each sex) to avoid high larval densities. Adult flies were allowed to lay eggs for 1 d, then transferred to new vials for an additional day, then discarded. To encourage remating, male and female parents were separated at the first transfer, and placed in vials with opposite-sex flies from a different vial. When flies began to eclose, virgins were collected at 8-h intervals and separated by sex. Virgins were kept in vials with no more than 10 females or 15 males until imaging.

In a second set of populations, we attempted to generate more efficient selection on the allometric slope by increasing the variance in size, potentially reducing the sampling variance in the estimation of the allometric slope. This was achieved by subjecting half the larvae in those populations to a starvation treatment, similar to that of Stillwell et al. (48). Larvae prevented from feeding after they reach a critical size for pupariation (approximately the start of the third larval instar) can eclose, but forego the most rapid period of growth, resulting in very small adults; following starvation, adults can have a thorax length as small as half the average size of fully fed flies. Thus, combining starved and normally reared flies greatly increases the variance in size among flies. Each generation, the selected adult flies in the starved populations were split evenly into two groups: One half was allowed to lay eggs in vials as described above, and their larvae were fed throughout the larval phase. The other half was confined overnight in a 90-mm Petri dish with standard food medium, during which time they mated and laid eggs. The following day, adults were removed from these egg layers, and the Petri dishes were placed in an incubator for 4–6 d. The dishes were checked regularly, and when most of the larvae appeared to have reached critical size for survival to adulthood, they were removed from the dish and placed in vials containing agar only, with no more than 20 larvae per vial. These larvae continued to consume the nonnutritive agar medium for several days before pupariation.

Because the timing of development varied greatly among the selected populations, we used the average size as determined by visual inspection to determine when the larvae had reached the critical size. Equal numbers of adults from starvation and normal treatments were imaged in the starved populations.

Later in the course of the experiment, the fecundity of the two replicate starved slope-selected populations decreased. To counter this, we induced females to lay more eggs by removing the males from egg layers after the first day and replacing them with mated females from a stock bearing the Tubby (*Tb*) and white (*w*) mutations. The increased density of ovipositing females encouraged further egg laying by the selected females. The *Tb* phenotype enabled us to identify and remove the mutant larvae; mutant adults that remained were identified by the *w* eye color mutation and removed. Even with this method, however, we were sometimes unable to collect the full 200 virgin flies from each population toward the end of the experiment.

Justification of the Allometric Slope Selection Index. We developed a selection index based on Huxley's allometric model. Huxley (5) showed that a trait's size (*Y*) relates to body size (*X*) by an allometric relation if both trait size and body size depend on some common growth variable *G*, such that $dX/dt = uXG$ and $dY/dt = vYG$, where *u* and *v* are specific constants for body size and trait size, respectively, and *t* is the time of growth. Solving these differential equations for *X* and *Y* at some developmental stage (e.g., *t* = adult) gives the power functions

$$\begin{aligned} X &= X_0 Q^u, \\ Y &= Y_0 Q^v, \end{aligned}$$

where *X*₀ and *Y*₀ are initial values for *X* and *Y*, and *Q* is *G* integrated over [*t* = 0, *t* = adult]. Transforming these power functions to the natural log scale gives

$$\begin{aligned} x &= x_0 + uq, \\ y &= y_0 + vq, \end{aligned}$$

where the lowercase letters *x*, *y*, and *q* are used to indicate log_e-transformed variables. From this, we get the allometric equation

$$y = \log_e[a] + bx,$$

where the allometric slope $b = v/u$, and the allometric intercept $\log_e[a] = y_0 - bx_0$. We are interested in selecting on the ratio v/u . Assuming that *u* and *v* as well as relative fitness (*w*) are multivariate normally distributed with no correlation between *u* and *v*, the selection differential of the ratio $b = v/u$ is given by

$$\begin{aligned} S[b] &= \text{Cov}\left[\frac{v}{u}, w\right] \\ &= \text{Cov}\left[\frac{1}{u}, w\right] \bar{v} + E\left[\frac{1}{u}(v - \bar{v})(w - 1)\right] \\ &\approx \frac{1}{\bar{u}} \left(\text{Cov}[v, w] - E\left[\frac{1}{u}\right] \text{Cov}[u, w] \right) \\ &= \frac{1}{\bar{u}} (S[v] - \bar{b}S[u]), \end{aligned}$$

where $E[\cdot]$ or one overbar denotes the expectation, $S[v] = \text{Cov}[v, w]$, $S[u] = \text{Cov}[u, w]$, and $\bar{b} = E[v/u]$. The approximation is from the Taylor series $1/u \approx 1/\bar{u} - (u - \bar{u})/\bar{u}^2$, and is a good approximation

when the coefficient of variation (CV) of u is small. From this, we see that the selection differential on v/u is proportional to the selection differential on v ($S[v]$) minus the selection differential on u ($S[u]$) weighted by the average allometric slope. To obtain these selection differentials, we use the standard quadratic relative fitness function $w = \mu + \beta_x x + \beta_y y + \frac{1}{2}\gamma_x x^2 + \frac{1}{2}\gamma_y y^2 + \gamma_{xy} xy$, where μ is the intercept and β_x , β_y , γ_x , γ_y , and γ_{xy} can be interpreted as the standard linear and quadratic selection gradients of x and y . We scale so that $\bar{x} = 0$ and $\bar{y} = 0$; the selection differentials $S[v]$ and $S[u]$ as functions of the selection gradients are then given by

$$\begin{aligned} S[v] &= \text{Var}[q] \text{Var}[v] (\gamma_y + \bar{u} \gamma_{xy}), \\ S[u] &= \text{Var}[q] \text{Var}[u] (\gamma_x + \bar{v} \gamma_{xy}). \end{aligned}$$

Substituting this into the equation for the selection differential on b , we obtain

$$S[b] = \frac{1}{\bar{u}} \text{Var}[q] \left(\text{Var}[v] \gamma_y - \bar{b} \text{Var}[u] \gamma_x + \bar{u} \left(\text{Var}[v] - \bar{b}^2 \text{Var}[u] \right) \gamma_{xy} \right). \quad \text{[S1]}$$

This equation shows that disruptive selection on y (positive γ_y) and stabilizing selection on x (negative γ_x) both select for increased allometric slope. A positive correlational selection gradient (γ_{xy}), on the other hand, contributes to increased allometric slope only when

$$\text{Var}[v] > \bar{b}^2 \text{Var}[u].$$

This is because the correlational selection generates a selection differential both on $\text{Cov}[x, y]$ and on $\text{Var}[x]$. Assuming that the average allometric slope (\bar{b}) equals the ratio $\text{Cov}[x, y]/\text{Var}[x]$, we can simplify Eq. S1 by ensuring that there is no selection on $\text{Var}[x]$. To accomplish this, we use the following argument from standard quantitative genetic theory: We know that the selection differential of the phenotypic covariance matrix ($S[\mathbf{P}]$), when there is no linear selection, is given by $S[\mathbf{P}] = \mathbf{P}\boldsymbol{\gamma}\mathbf{P}$, where $\boldsymbol{\gamma}$ is the matrix of quadratic selection gradients. Under the assumption of multivariate normality, we can derive the selection differential of the variance of x ,

$$S[\text{Var}[x]] = \text{Var}[x]^2 \gamma_x + 2\text{Var}[x] \text{Cov}[x, y] \gamma_{xy} + \text{Cov}[x, y] \gamma_y.$$

This shows that there is no selection differential on the variance of x ($S[\text{Var}[x]] = 0$) when $\gamma_x = -2\bar{b}\gamma_{xy}$ and $\gamma_y = 0$. Substituting $\gamma_x = -2\bar{b}\gamma_{xy}$ and $\gamma_y = 0$ into Eq. S1 gives

$$S[b] = \text{Var}[q] \left(\bar{b}^2 \text{Var}[u] \left(\frac{2}{\bar{u}} - 1 \right) + \text{Var}[v] \right) \gamma_{xy}.$$

Biologically realistic values of u are less than 1 and certainly not higher than 2, because the amount of resources allocated to X is most likely a diminishing function of the total amount of resources available (Q). This means that this selection differential of the allometric slope is proportional to γ_{xy} when there is no selection on the variance of x .

The average individual allometric slope (\bar{b}) in the above models relates to the observed static allometric slope, $b_{\text{static}} = \text{Cov}[x, y]/\text{Var}[x]$, in the same way as the average ontogenetic allometric slope relates to the static allometric slope (see ref. 23). In essence, this means a change in \bar{b} is expected to give the same change in b_{static} , and that $\bar{b} = b_{\text{static}}$ if both the individual allometric intercept ($\log_e[a]$) and slope (b) are uncorrelated with size (x).

Based on the above results, we constructed the selection index for the slope as

$$W_{\text{slope}} = \beta_x (x - \bar{x}) + \beta_y (y - \bar{y}) + \frac{1}{2} \gamma_x (x - \bar{x})^2 + \gamma_{xy} (x - \bar{x})(y - \bar{y}),$$

where $\gamma_{xy} = 1$ for the up selection (increase in slope) and -1 for the down selection (decrease in slope). We did not directly use $\beta_x = 0$, $\beta_y = 0$, and $\gamma_x = -2\bar{b}\gamma_{xy}$, because it is unlikely that the sample distribution is perfectly multivariate normal. Instead, the function (W_{slope}) was optimized for the parameters β_x , β_y , and γ_x , to generate as little selection as possible on the means of x and y and on the variance of x .

Selection Procedure. For the intercept selection, we wanted the average size of the selected individuals to be as similar as possible to the average size of all individuals in the population (i.e., no selection on size). To do this, we searched a wide range of values of β_1 to find the value that minimized the value of $(S[x])^2$, where β_1 is the directional selection gradient on size and $S[x]$ is the selection differential on size (i.e., the difference between the mean size of the selected individuals and the mean size of all individuals in the population).

For the slope selection, the optimization was done in three rounds to estimate the parameters β_x , β_y , and γ_x . First, we searched through a range of different values for γ_x with $\beta_x = 0$ and $\beta_y = 0$, to minimize $(S[\text{Var}[x]])^2$, where $S[\cdot]$ denotes the selection differential. Next, we searched through a wide range of combinations of values of β_x and β_y to minimize $(S[x]/\bar{x})^2 + (S[y]/\bar{y})^2$ with γ_x at its current optimized value [i.e., the value that gave the lowest $(S[\text{Var}[x]])^2$]. Finally, we did a second round of searching through different values of γ_x to minimize $(S[\text{Var}[x]])^2$, but this time with β_x and β_y at the optimized values.

Statistical Analyses of the Comparative Data. To estimate the rate of evolution for the allometric intercept, we fitted a Brownian-motion model of evolution using the phylogenetic mixed model (46)

$$y_{ijk} = u_i + b_i x_{ij\bullet} + a_j + \varepsilon_{ijk},$$

where y is \log_e L2 length, x is \log_e wing size (square root of wing area), u is the common intercept for each sex, b is the evolutionary allometric slope for each sex, a is the phylogenetic effect, and ε is the residual term. The subscripts i , j , and k , represent sex, species, and individual, respectively, and subscript \bullet means the average taken over the indicated level. The residuals are assumed to be independent identically normally distributed, whereas the phylogenetic effects are assumed to be distributed as $\mathbf{a} \sim N(0, \sigma_{\text{rate}}^2 \mathbf{A})$, where \mathbf{A} is a phylogenetic relatedness matrix in which the elements are the shared branch length of species scaled to unit depth. This matrix was computed from a published phylogeny (42) with two species added based on other published evidence: *Drosophila arizonae* (41) and *D. athabasca* (49). Note that six species were not included in this analysis because they were not in our phylogeny (*Homoneura* sp., *Leucophenga* sp., *Monochaetoscinella* sp., *Neogriphoneura sordida*, *Samoia leonensis*, and *Thaumatomyia* sp.). The rate (increase in variance) per million years is given by σ_{rate}^2/t , where t is the depth of the phylogeny in millions of years. Because the depth of this phylogeny is highly uncertain (47), we used both a ‘‘best guess’’ of 133 million years and a conservative estimate of 50 million years to estimate the rate.

To estimate the rate of evolution for the allometric slope, we fitted a similar model as for the intercept,

$$y_{ijk} - y_{ij\bullet} = b_i (x_{ijk} - x_{ij\bullet}) + a_j (x_{ijk} - x_{ij\bullet}) + \varepsilon_{ijk},$$

where b is the common within-species slope for each sex separately. The phylogenetic effects of the slope (a_j) are assumed to be distributed as the phylogenetic effects of the intercept, and

the residuals (ε_{ijk}) are assumed to be independent identically normally distributed. The per-million-year evolutionary rate for the slope was calculated in the same way as for the intercept.

The static allometric relationships within each sex for each species, presented in Fig. 1, were estimated by standard linear regression models with \log_e L2 length as the response variable and \log_e wing size as the explanatory variable. The evolutionary allometry for each sex was a linear regression on the species means with \log_e L2 length as response and \log_e wing size as predictor.

Statistical Analyses of the Selection Experiment. Changes and differences in allometric intercept and slope of \log_e vein L2 length on \log_e wing size (square-root wing area) were analyzed by a series of linear mixed-effects models because of the hierarchical structure of the data.

For the selection on the intercept, we wanted to estimate the following parameters: the average wing size (intercept) in the starting generation for each sex i (u_i), the average allometric slope for each sex (b_i), the linear change per generation of the intercept for all treatments j (up selected, down selected, and control) nested within sex (a_{1ij}), the quadratic response to selection of the intercept for the up- and down-selection treatment for each sex separately (a_{2ij}), and the linear effect of relaxed selection on the intercept for the up and down selection treatment for each sex separately (a_{3ij}). To estimate these parameters, we fitted a broken-stick mixed model with \log_e vein L2 length (y_{ijklm}) as a function of \log_e wing size centered within sex ($x_{ijklm} - x_{i\bullet\bullet\bullet}$) and generation (t),

$$y_{ijklm} = u_i + b_i(x_{ijklm} - x_{i\bullet\bullet\bullet}) + a_{1ij}t_1 + a_{2ij}t_1^2K + a_{3ij}t_2K + c_{ijk}t_1 + d_{ijkl} + \varepsilon_{ijklm},$$

where subscripts k , l , and m denote population (nested within treatment), generation (nested within population), and individual, respectively. Subscript \bullet means the average taken over the indicated level. We implemented the broken-stick regression model through the values of t_1 and t_2 : t_1 represents generations 0–7 for the selected populations (treatment up and down) and generations 0–23 for the controls. For the selected populations, t_1 takes the values 0–7 for generations 0–7 and value 0 for generations 8–23. For the controls, t_1 takes the values 0–23 for generations 0–23. The other generation variable, t_2 , represents generations 8–23; t_2 takes the values 0 for generations 0–7 and 0–15 for generations 8–23. The indicator variable K takes the value 0 for the control treatment and 1 for the up and down selection treatments. We also included two random effects (c_{ijk} and d_{ijkl}). The first random effect, c_{ijk} , is the deviation of each replicated population nested within treatment from the rest of the model, assumed to be independent identically normally distributed. The second random effect, d_{ijkl} , is the deviation of each generation (nested within population) from the rest of the model. This second random effect is assumed to be multivariate normally distributed with a variance term multiplied with a relatedness matrix (\mathbf{A}) to account for temporal autocorrelation. The diagonal elements of \mathbf{A} are unity, and the off-diagonal elements are given by $0.5^{\Delta t}$, where Δt is the difference in number of generations for elements of \mathbf{A} belonging to the same population, and zero for all other elements. The residuals (ε_{ijklm}), the deviation of each individual fly from the model prediction, are assumed to be independent identically normally distributed.

For the selection on the slope, we wanted to estimate the following parameters: the common allometric slope for all treatments in the starting generation for each sex i separately (b_i) and the linear change in allometric slope per generation t for each treatment j (up selected, down selected, and control) nested within sex (a_{ij}). To estimate these parameters, we used a random

regression model where we used \log_e vein L2 length centered on the within-generation sex mean for each population k ($y_{ijklm} - y_{ijkl}$) as response variable, and \log_e wing size within-generation sex mean for each population k ($x_{ijklm} - x_{ijkl}$) and generation (t) as explanatory variables,

$$y_{ijklm} - y_{ijkl} = b_i(x_{ijklm} - x_{ijkl}) + a_{ij}(x_{ijklm} - x_{ijkl})t + c_{ijk}(x_{ijklm} - x_{ijkl})t + d_{ijkl}(x_{ijklm} - x_{ijkl}) + \varepsilon_{ijklm},$$

where the subscripts denote the same as in the model for selection on the intercept. The random effects c_{ijk} give the deviation to the treatment mean in the change of the allometric slope for each population (nested within treatment), d_{ijkl} gives the deviation in the allometric slope from the rest of the model for each generation l (nested within population), and ε_{ijklm} is the residual deviation of each fly. The random effects are assumed to be independent identically normally distributed, except d_{ijkl} , which is distributed as d_{ijkl} in the model for the intercept.

Separate analyses of the unstarved and the starved populations were conducted using this model.

For the change in slope after selection in the unstarved populations, we wanted to estimate the following parameters: the average slope in the first generation for each treatment j (up and down selected) nested within sex i (b_{ij}), the linear change in the allometric slope per generation of random mating t for each treatment nested within sex (a_{1ij}), and the change in allometric slope per generation of random mating due to breakup of linkage disequilibrium for each treatment nested within sex (a_{2ij}). We fitted the following random regression model:

$$y_{ijklm} - y_{ijkl} = b_{ij}(x_{ijklm} - x_{ijkl}) + a_{1ij}(x_{ijklm} - x_{ijkl})t + a_{2ij}(x_{ijklm} - x_{ijkl})(1 - r^t) + c_{ijk}(x_{ijklm} - x_{ijkl}) + d_{ijkl}(x_{ijklm} - x_{ijkl}) + \varepsilon_{ijklm},$$

where the subscripts denote the same as in the model for the selection on the intercept. The effect of linkage disequilibrium is a linear function of $1 - r^t$, where r is the average recombination fraction, 0.365 in *D. melanogaster* (37), and t is number of generations of random mating. Hence, by including breakup of linkage disequilibrium as a linear effect in our model, we obtain an estimate of the asymptote at linkage equilibrium. The random effect c_{ijk} gives the deviation of the treatment mean allometric slope for each population (nested within treatment), d_{ijkl} gives the deviation in the allometric slope from the rest of the model for each generation l (nested within population), and ε_{ijklm} is the residual deviation of each fly. The random effects are assumed to be independent identically normally distributed.

To estimate the maximum fraction of the selection response that was due to linkage disequilibrium in each sex (q_i), we replaced the term $a_{2ij}(x_{ijklm} - x_{ijkl})(1 - r^t)$ in the above random regression model with $q_i(x_{ijklm} - x_{ijkl})(1 - r^t)K$. In this model, the selection response in all treatments is scaled to 1 by using the scaling factor K with values 0.327 and 0.365 for the females and males, respectively, in the up-selection treatment, and -0.190 and -0.182 for the females and males, respectively, in the down-selection treatment. The value of K is the difference between the allometric slope in the starting generation and after selection ended (generation 0 of relaxed selection). Hence, the parameter q_i is an estimate of the maximum average fraction of the total selection response that is consistent with linkage disequilibrium across treatments. The reason that this is the maximum fraction is that natural selection in the laboratory environment could also cause exponential decay.

To investigate the effect of starvation on the evolved slopes, we subjected some of the larvae of the unstarved populations to the starvation treatment one generation after selection ended. We estimated the difference in allometric slope between the up- and

down-selected populations both for starved and nonstarved flies using analysis of covariance.

All analyses were done in R (50) using the packages lme4 (51) and pedigreemm (52).

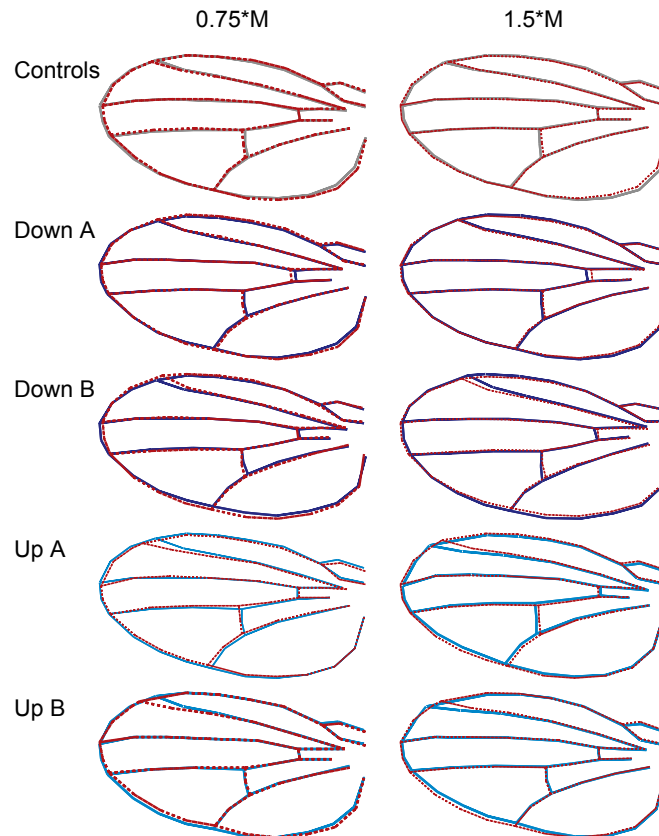


Fig. S1. Change in wing shape with size (allometry) of the controls and the slope-selected populations relative to the isometric expectation (dotted red lines). The two replicated down-selected populations are denoted “Down A” and “Down B,” and the two replicated up-selected populations are denoted “Up A” and “Up B.” Shapes were constructed as point estimates of multivariate regressions of shape (i.e., 58 shape variables) on wing area evaluated at standard values given by $0.75\times$ median size of each population (*Left*) and $1.5\times$ median size of each population (*Right*), then averaged over sexes and generations 21–24. Isometric expectation is based on the shape at median size of each population, scaled by $0.75\times$ and $1.5\times$ at the lower and upper end, respectively. In the control, the allometric relationship was slightly above 1, making the position of the landmark 4 (see Fig. S3) more proximal in small wings than in large wings (position on each side of the isometric expectation). The decrease in the allometric slope in the down-selected populations reverses this effect; landmark 4 becomes more distal in small wings and more proximal in large wings. In the up-selected populations where the allometric slope is increased, the normal trend is amplified, with landmark 4 becoming even more proximal in small wings and even more distal in large wings.

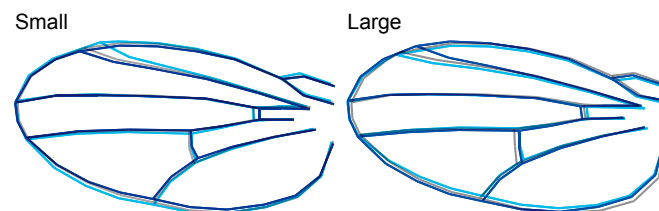


Fig. S2. Response of wing-shape allometry to selection on the allometric slope. The image on the *Left* represents the mean shape of wings that are $0.75\times$ the median wing area, and the image on the *Right* represents the mean shapes of wings that are $1.5\times$ the median wing area. Control is in gray and average response of up-selected populations are in light blue and of down-selected populations are in dark blue. Shapes were constructed as in Fig. S1, but using the median of the control as reference and averaged over replicated populations in addition to sexes and generations. All contours were scaled to the same size to facilitate visualization of shape differences. The direct response to selection is best seen for the change in position of landmark 4 (see Fig. S3) relative to the control. In up-selected populations with increased allometric slope, the position of landmark 4 is more distal in small wings and more proximal in large wings relative to the control, whereas the opposite pattern is apparent in the down-selected populations with decreased allometric slope.

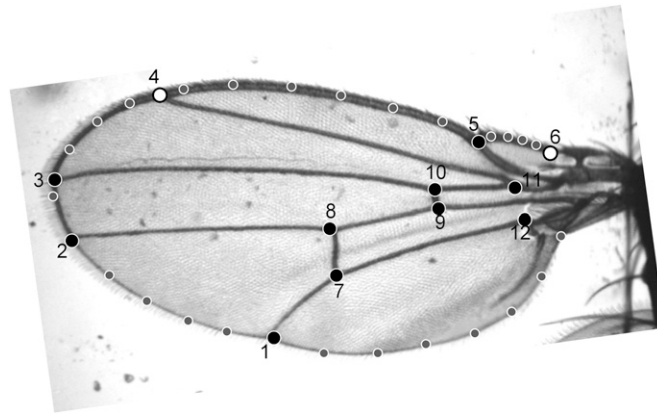


Fig. S3. Picture of a *D. melanogaster* wing with landmarks. The 12 numbered landmarks are vein intersections and the humeral break in the costa (landmark 6). The landmarks in gray are semilandmarks evenly spaced between each pair of landmarks on the outline. We used the distance between landmarks 4 and 6 as a measure of L2 length. Landmark 11 was not used because it is much less precisely estimated than landmark 6. In the selected *D. melanogaster* populations, area was estimated using the surveyor's formula as the polygon bounded by landmark 6, the juncture of the costa with the vein L1, and the notch between the wing blade and alula; six evenly spaced semilandmarks along the costa between the first two landmarks; and 24 evenly spaced semilandmarks along the wing margin between the latter two landmarks. For the comparative data, we calculated wing area using the surveyor's formula on the convex hull of a set of 16 evenly spaced points along the spline curve of the wing outline, plus the landmark defining the humeral break. We used the square root of wing area as measure of wing size.

Table S1. Estimated evolutionary rates for allometric intercepts and slope using a Brownian-motion model of evolution

Parameter	Rate	95% confidence interval	Unit
Depth of phylogeny 50 My			
Allometric intercept	0.00180	0.00130–0.00241	$(\log_e \text{ mm})^2/\text{My}$
Allometric slope	0.00138	0.00095–0.00196	slope^2/My
Depth of phylogeny 133 My			
Allometric intercept	0.00068	0.00049–0.00091	$(\log_e \text{ mm})^2/\text{My}$
Allometric slope	0.00052	0.00036–0.00074	slope^2/My

The depth of the phylogeny is highly uncertain; we therefore give the rates for phylogenies of two depths (50 My or 133 My). The unit denoted slope is the proportional change in vein L2 length for a proportional change in wing size, $(\log_e \text{ mm})/(\log_e \text{ mm})$, or the elasticity of vein L2 length to wing size. Note that the rates are given as increase in variance of traits over time. In *Results and Discussion*, we give the square root of the rates (standard deviations), to increase interpretability. Because the intercept is on the natural log scale, the standard deviation is approximately the coefficient of variation, and multiplying these values by 100 scales them as percent of the trait mean.

Table S2. Allometric parameters and the change in intercept during the intercept-selection experiment

Parameter	Estimate	SE	Unit
Males			
Common intercept at $t = 0$	0.29520	0.00276	\log_e mm
Linear change per generation Control at $t = 0-23$	-0.00025	0.00018	$(\log_e \text{ mm})/t$
Linear change per generation Up Selection at $t = 0-7$	0.01998	0.00310	$(\log_e \text{ mm})/t$
Linear change per generation Down Selection at $t = 0-7$	-0.01353	0.00310	$(\log_e \text{ mm})/t$
Quadratic change per generation Up Selection at $t = 0-7$	-0.00114	0.00046	$(\log_e \text{ mm})/t^2$
Quadratic change per generation Down Selection at $t = 0-7$	0.00059	0.00046	$(\log_e \text{ mm})/t^2$
Linear change per generation Up Selection at $t = 7-23$	-0.00136	0.00059	$(\log_e \text{ mm})/t$
Linear change per generation Down Selection at $t = 7-23$	0.00014	0.00059	$(\log_e \text{ mm})/t$
Common static allometric slope	1.07830	0.00739	slope
Females			
Common intercept at $t = 0$	0.45481	0.00276	\log_e mm
Linear change per generation Control at $t = 0-23$	-0.00053	0.00018	$(\log_e \text{ mm})/t$
Linear change per generation Up Selection at $t = 0-7$	0.01603	0.00310	$(\log_e \text{ mm})/t$
Linear change per generation Down Selection at $t = 0-7$	-0.01617	0.00310	$(\log_e \text{ mm})/t$
Quadratic change per generation Up Selection at $t = 0-7$	-0.00069	0.00046	$(\log_e \text{ mm})/t^2$
Quadratic change per generation Down Selection at $t = 0-7$	0.00084	0.00046	$(\log_e \text{ mm})/t^2$
Linear change per generation Up Selection at $t = 7-23$	-0.00136	0.00059	$(\log_e \text{ mm})/t$
Linear change per generation Down Selection at $t = 7-23$	0.00030	0.00059	$(\log_e \text{ mm})/t$
Common static allometric slope	1.09650	0.00736	slope

Generation is denoted t , and the unit denoted slope is the proportional change in vein L2 length for a proportional change in wing size.

Table S3. Allometric slopes and their change during the slope-selection experiment

Parameter	Estimate	SE	Unit
Males			
Common slope at $t = 0$	1.08186	0.02145	slope
Linear change per generation Up Selection	0.01185	0.00561	slope/ t
Linear change per generation Down Selection	-0.00939	0.00561	slope/ t
Linear change per generation Control	0.00062	0.00570	slope/ t
Females			
Common slope at $t = 0$	1.09302	0.02139	slope
Linear change per generation Up Selection	0.01265	0.00561	slope/ t
Linear change per generation Down Selection	-0.01185	0.00561	slope/ t
Linear change per generation Control	0.00126	0.00570	slope/ t

See Table S2 for explanation of units.

Table S4. Allometric slopes and their change during relaxed selection in the slope-selection experiment

Parameter	Estimate	SE	Unit
Males			
Initial slope Up Selection	1.43663	0.05860	slope
Initial slope Down Selection	0.89016	0.05897	slope
Total change due to LD Up Selection	-0.06487	0.09414	slope/ $(1 - r^d)$
Total change due to LD Down Selection	0.05153	0.09318	slope/ $(1 - r^d)$
Linear change per generation Up Selection	-0.01614	0.00655	slope/ t
Linear change per generation Down Selection	0.00499	0.00633	slope/ t
Females			
Initial slope Up Selection	1.40965	0.05661	slope
Initial slope Down Selection	0.89304	0.05902	slope
Total change due to LD Up Selection	-0.02268	0.09194	slope/ $(1 - r^d)$
Total change due to LD Down Selection	0.06968	0.09429	slope/ $(1 - r^d)$
Linear change per generation Up Selection	-0.01272	0.00633	slope/ t
Linear change per generation Down Selection	0.00670	0.00646	slope/ t

The constant r is the average recombination fraction in *Drosophila melanogaster* (0.365); LD, linkage disequilibrium. See Table S2 for explanation of units.

Table S5. Allometric slopes and their change in the slope-selected populations subjected to the starvation treatment

Parameters	Estimate	SE	Unit
Males			
Common slope at $t = 0$	1.13597	0.00991	slope
Linear change per generation Control	-0.00075	0.00146	slope/t
Linear change per generation Up Selection	-0.00063	0.00139	slope/t
Linear change per generation Down Selection	-0.00193	0.00140	slope/t
Females			
Common slope at $t = 0$	1.12814	0.00966	slope
Linear change per generation Control	0.00028	0.00145	slope/t
Linear change per generation Up Selection	-0.00059	0.00137	slope/t
Linear change per generation Down Selection	-0.00169	0.00139	slope/t

See Table S2 for explanation of units.

Table S6. Taxa included with total sample size (N)

Family	Genus	Species (subspecies)*	Location of collection	Source [†]	Flies [‡]	N
Chloropidae	<i>Monochaetoscinella</i>	Sp.	Tallahassee, FL	Coll.	Wild	48
Chloropidae	<i>Thaumatomyia</i>	Sp.	Tallahassee, FL	Coll.	Wild	22
Drosophilidae	<i>Chymomyza</i>	<i>procnemis</i>	Oahu, HI; Georgia	SS 20000–2631.1	Lab	120
Drosophilidae	<i>Dettopsomyia</i>	<i>nigrovittata</i>	Tallahassee, FL	Coll.	Wild	15
Drosophilidae	<i>Drosophila</i>	<i>acutilabella</i>	Tallahassee, FL	Coll.	Wild, F1	205
Drosophilidae	<i>Drosophila</i>	<i>affinis</i>	Tallahassee, FL	Coll.	Lab	209
Drosophilidae	<i>Drosophila</i>	<i>algonquin</i>	Michigan, OH	Coll.	Lab (wild)	237
Drosophilidae	<i>Drosophila</i>	<i>americana</i> (<i>americana</i>)	Chinook, MT	SS 15010–0951.2	Lab	109
Drosophilidae	<i>Drosophila</i>	<i>americana</i> (<i>texana</i>)	Morrilton, AR	SS 15010–1041.23	Lab	215
Drosophilidae	<i>Drosophila</i>	<i>ananassae</i>	Tallahassee area, FL; south Georgia	Coll.	Lab	235
Drosophilidae	<i>Drosophila</i>	<i>arizonae</i>	Riverside, CA; Baja California, Mexico; Tucson, AZ	Laura Reed	Lab	275
Drosophilidae	<i>Drosophila</i>	<i>athabasca</i>	Toronto, ON, Canada	Coll.	Lab	79
Drosophilidae	<i>Drosophila</i>	<i>azteca</i>	Lassen, CA	Coll.	Lab	49
Drosophilidae	<i>Drosophila</i>	<i>bifasciata</i>	Maggia, Ticino, Switzerland	SS 14012–0181.1	Lab	217
Drosophilidae	<i>Drosophila</i>	<i>busckii</i>	Tallahassee, FL	Coll.	Wild, F1	105
Drosophilidae	<i>Drosophila</i>	<i>cardini</i>	Tallahassee area, FL	Coll.	Lab	210
Drosophilidae	<i>Drosophila</i>	<i>elegans</i>	India	J. David	Lab	215
Drosophilidae	<i>Drosophila</i>	<i>emarginata</i>	Huatusco, Veracruz, Mexico	SS 14042–0841.6	Lab	232
Drosophilidae	<i>Drosophila</i>	<i>equinoxialis</i>	Panama	Coll.	Lab	214
Drosophilidae	<i>Drosophila</i>	<i>erecta</i>	unknown	SS 14021–0224.0	Lab	193
Drosophilidae	<i>Drosophila</i>	<i>eugracilis</i>	Palawan, Philippines	SS 14026–0451.1	Lab	212
Drosophilidae	<i>Drosophila</i>	<i>euronotus</i>	Tallahassee, FL	Coll.	F1, Lab (wild)	296
Drosophilidae	<i>Drosophila</i>	<i>falleni</i>	Tallahassee, FL	Coll.	F1, F2 (wild)	277
Drosophilidae	<i>Drosophila</i>	<i>figusphila</i>	Khan-ing Tong, Taiwan	SS 14025–0441.1	Lab	226
Drosophilidae	<i>Drosophila</i>	<i>aff. florum</i>	Tallahassee, FL	Coll.	Wild, F1	210
Drosophilidae	<i>Drosophila</i>	<i>funnebris</i>	Pentwater, MI	Coll.	Lab (wild)	216
Drosophilidae	<i>Drosophila</i>	<i>gaucha</i>	Montevideo, Uruguay	J. David	Lab	209
Drosophilidae	<i>Drosophila</i>	<i>greeni</i>	Africa	J. David	Lab	206
Drosophilidae	<i>Drosophila</i>	<i>guanche</i>	Tenerife, Canary Islands	SS 14011–0095.0	Lab	209
Drosophilidae	<i>Drosophila</i>	<i>guttifera</i>	Tallahassee, FL	Coll.	Wild, F1	99
Drosophilidae	<i>Drosophila</i>	<i>hydei</i>	Tallahassee, FL	Coll.	Lab	134
Drosophilidae	<i>Drosophila</i>	<i>immigrans</i>	Tallahassee, FL	Coll.	Lab	164
Drosophilidae	<i>Drosophila</i>	<i>kikkawai</i>	India	J. David	Lab	213
Drosophilidae	<i>Drosophila</i>	<i>lucipennis</i>	Chi-tou, Taiwan; Wulai, Taiwan	SS 14023–0331.0; 14023–0331.1	Lab	245
Drosophilidae	<i>Drosophila</i>	<i>macrospina</i>	Tallahassee, FL	Coll.	Wild, F1, F2	72
Drosophilidae	<i>Drosophila</i>	<i>malerkotliana</i>	Tallahassee, FL	Coll.	Lab	220
Drosophilidae	<i>Drosophila</i>	<i>mauritiana</i>	Mauritius	J. David	Lab	203
Drosophilidae	<i>Drosophila</i>	<i>melanica</i>	Patagonia, AZ; northern Florida and southern Georgia	SS 15030–1141.2	Lab	267
Drosophilidae	<i>Drosophila</i>	<i>melanogaster</i>	Wabasso, FL	Coll.	Wild	247
Drosophilidae	<i>Drosophila</i>	<i>mercatorum</i>	Asheville, NC	Coll.	Lab	209
Drosophilidae	<i>Drosophila</i>	<i>micromelanica</i>	Smithville, TX	SS 15030–1151.1	Lab	155
Drosophilidae	<i>Drosophila</i>	<i>mimetica</i>	Southeast Asia	John True	Lab	19
Drosophilidae	<i>Drosophila</i>	<i>mojavensis</i>	Baja California, Mexico; California	Laura Reed	Lab	163
Drosophilidae	<i>Drosophila</i>	<i>mulleri</i>	central-east Florida	Coll.	Lab	195
Drosophilidae	<i>Drosophila</i>	<i>nasuta</i>	Gabon, Africa	J. David	Lab	196
Drosophilidae	<i>Drosophila</i>	<i>nebulosa</i>	south Florida	Coll.	Lab	212
Drosophilidae	<i>Drosophila</i>	<i>neocordata</i>	Minas Gerais, Brazil	SS 14041–0831.0	Lab	217
Drosophilidae	<i>Drosophila</i>	<i>neotestacea</i>	Rochester, NY; northern Georgia	Coll.	Lab; Wild, F1	208
Drosophilidae	<i>Drosophila</i>	<i>nigromelanica</i>	Tallahassee, FL	Coll.	Wild, F1	204
Drosophilidae	<i>Drosophila</i>	<i>nikanano</i>	Ivory Coast	SS 14028–0601.0	Lab	209
Drosophilidae	<i>Drosophila</i>	<i>occidentalis</i>	Madera County, CA	Coll.	Wild, F1, F2	205
Drosophilidae	<i>Drosophila</i>	<i>paramelanica</i>	Pentwater, MI; Smokemont, NC	SS 15030–1161.2	Lab	323
Drosophilidae	<i>Drosophila</i>	<i>pauistorum</i>	Central America	SS 14030–0771.13	Lab	201
Drosophilidae	<i>Drosophila</i>	<i>peninsularis</i>	central Florida	Coll.	Lab	206
Drosophilidae	<i>Drosophila</i>	<i>persimilis</i>	Mount St. Helena, CA	Jody Hey	Lab	55
Drosophilidae	<i>Drosophila</i>	<i>pictiventris</i>	Great Inagua, Bahamas	SS 12000–0072.0	Lab	112

Table S6. Cont.

Family	Genus	Species (subspecies)*	Location of collection	Source [†]	Flies [‡]	N
Drosophilidae	<i>Drosophila</i>	<i>pinicola</i>	Lassen, CA	Coll.	Lab	202
Drosophilidae	<i>Drosophila</i>	<i>pseudoobscura</i> (<i>bogotana</i>)	Sutatausa, Susa, Potosi, Colombia	Jody Hey	Lab	73
Drosophilidae	<i>Drosophila</i>	<i>pseudoobscura</i> (<i>pseudoobscura</i>)	Tucson, AZ	SS 14011–0121.0	Lab	198
Drosophilidae	<i>Drosophila</i>	<i>putrida</i>	Tallahassee, FL	Coll.	Wild, F1	210
Drosophilidae	<i>Drosophila</i>	<i>recens</i>	Calamity Pond, NY; Deer Isle, ME; Big Moose, NY	Coll.	Lab	224
Drosophilidae	<i>Drosophila</i>	<i>repleta</i>	Tallahassee, FL	Coll.	Wild, F1, Lab	217
Drosophilidae	<i>Drosophila</i>	<i>robusta</i>	Tallahassee, FL	Coll.	Lab	101
Drosophilidae	<i>Drosophila</i>	<i>saltans</i>	San Jose, Costa Rica	SS 14045–0911.0	Lab	181
Drosophilidae	<i>Drosophila</i>	<i>santomea</i>	Sao Tome y Principe	SS	Lab	205
Drosophilidae	<i>Drosophila</i>	<i>sechellia</i>	Seychelles	J. David	Lab	210
Drosophilidae	<i>Drosophila</i>	<i>seguyi</i>	Africa	J. David	Lab	210
Drosophilidae	<i>Drosophila</i>	<i>simulans</i>	Tallahassee, FL	Coll.	Lab	195
Drosophilidae	<i>Drosophila</i>	<i>stalkerii</i>	Guantanamo Bay, Cuba	SS 15081–1451.10	Lab	203
Drosophilidae	<i>Drosophila</i>	<i>sturtevanti</i>	south Florida	Coll.	Wild, Lab	223
Drosophilidae	<i>Drosophila</i>	<i>subobscura</i>	Gif-sur-Yvette, France	G. Gilchrist	Gilchrist et al. (42)	69
Drosophilidae	<i>Drosophila</i>	<i>sulfurigaster</i> (<i>albostrigata</i>)	Siem Reap, Cambodia	SS 15112–1811.4	Lab	209
Drosophilidae	<i>Drosophila</i>	<i>sulfurigaster</i> (<i>bilimbata</i>)	Tantalus, Oahu, HI	SS 15112–1821.0	Lab	224
Drosophilidae	<i>Drosophila</i>	<i>sulfurigaster</i> (<i>sulfurigaster</i>)	Queensland, Australia	SS 15112–1831.0	Lab	210
Drosophilidae	<i>Drosophila</i>	<i>takahashii</i>	Nepal, Asia	SS 14022–0311.0	Lab	198
Drosophilidae	<i>Drosophila</i>	<i>testacea</i>	Germany	unknown	Lab	40
Drosophilidae	<i>Drosophila</i>	<i>tripunctata</i>	Tallahassee, FL; Pentwater, MI	Coll.	Wild, Lab	218
Drosophilidae	<i>Drosophila</i>	<i>virilis</i>	Pasadena, CA	SS 15010–1051.0	Lab	199
Drosophilidae	<i>Drosophila</i>	<i>willistoni</i>	northern Florida	Coll.	Lab	268
Drosophilidae	<i>Drosophila</i>	<i>yakuba</i>	Ivory Coast, Africa	SS 14021–0261.0;	Lab	209
Drosophilidae	<i>Hirtodrosophila</i>	<i>duncani</i>	Tallahassee, FL; Kalamazoo, MI	Coll.	F1, F2, Lab (wild)	219
Drosophilidae	<i>Hirtodrosophila</i>	Sp.	south Florida	Coll.	Lab	240
Drosophilidae	<i>Hirtodrosophila</i>	<i>thoracis</i>	Tallahassee area, FL	Coll.	Wild, F1	352
Drosophilidae	<i>Idiomyia</i>	<i>biseriata</i>	Mount Kaala, Oahu, HI	SS 15291–2551.1	Lab	210
Drosophilidae	<i>Idiomyia</i>	<i>crucigera</i>	Pupukea, Oahu, HI	SS 15287–2531.0	Lab	211
Drosophilidae	<i>Idiomyia</i>	<i>eurypeza</i>	Kumuwela, Kauai, HI	SS 15290–2581.0	Lab	210
Drosophilidae	<i>Idiomyia</i>	<i>grimshawi</i>	Auwahi, Maui, HI	SS 15287–2541.0	Lab	190
Drosophilidae	<i>Idiomyia</i>	<i>gymnobasis</i>	Auwahi, Maui, HI	SS 15284–2501.0	Lab	209
Drosophilidae	<i>Idiomyia</i>	<i>mimica</i>	Kipuka Ki, HI	SS 15292–2561.0	Lab	216
Drosophilidae	<i>Idiomyia</i>	<i>sooneae</i>	Pawaina, HI	SS 15290–2591.0	Lab	212
Drosophilidae	<i>Leucophenga</i>	Sp.	central Florida	Coll.	Wild	10
Drosophilidae	<i>Leucophenga</i>	<i>varia</i>	Tallahassee, FL	Coll.	Wild	29
Drosophilidae	<i>Mycodrosophila</i>	<i>claytonae</i>	Tallahassee area, FL	Coll.	Wild, F1	197
Drosophilidae	<i>Mycodrosophila</i>	<i>dimidiata</i>	Tallahassee area, FL	Coll.	Wild	208
Drosophilidae	<i>Samoia</i>	<i>leonensis</i>	Samoia	SS 80000–2761.03	Lab	201
Drosophilidae	<i>Scaptodrosophila</i>	<i>deflexa</i>	France	J. David	Lab	201
Drosophilidae	<i>Scaptodrosophila</i>	<i>dorsocentralis</i>	Japan	J. David	Lab	85
Drosophilidae	<i>Scaptodrosophila</i>	<i>latifasciaeformis</i>	north and central Florida	Coll.	Wild, Lab	204
Drosophilidae	<i>Scaptodrosophila</i>	<i>lebanonensis</i> (<i>casteeli</i>)	Veyo, Utah	SS 11010–0011.0	Lab	207
Drosophilidae	<i>Scaptodrosophila</i>	<i>lebanonensis</i> (<i>lebanonensis</i>)	Beirut, Lebanon	SS 11010–0021.0	Lab	211
Drosophilidae	<i>Scaptodrosophila</i>	<i>stonei</i>	Tehran, Iran	SS 11010–0041.1	Lab	210
Drosophilidae	<i>Scaptomyza</i>	<i>adusta</i>	north Florida; south Georgia	Coll.	Lab (wild)	235
Drosophilidae	<i>Scaptomyza</i>	<i>palmae</i>	Kahala Mountains, HI	SS 33000–2681.1	Lab	212
Drosophilidae	<i>Zaprionus</i>	<i>ghesquierei</i>	Gabon, Africa	J. David	Lab	224
Drosophilidae	<i>Zaprionus</i>	<i>indianus</i>	Brazil	J. David	Lab	208
Drosophilidae	<i>Zaprionus</i>	<i>inermis</i>	Koutaba, Cameroun	SS 50000–2746.0	Lab	148
Drosophilidae	<i>Zaprionus</i>	<i>sepsoides</i>	Kongo	SS 50000–2744.0	Lab	200
Drosophilidae	<i>Zaprionus</i>	Sg. <i>Anaprionus</i>	India	J. David	Lab	200

